

Decentralized High-Performance Control of DC Microgrids

Cheng Wang, Jiajun Duan, Bo Fan, Qinmin Yang, and Wenxin Liu

Abstract—Direct current (DC) microgrids have been widely used in many critical applications. Such systems avoid unnecessary AC/DC conversions and can simplify control design. To achieve high-performance control of such system, advanced control algorithm needs to be designed. This paper presents a novel decentralized output constrained control algorithm for single-bus DC microgrids. The control objectives are to realize high-performance control of DC bus voltage, user-defined load sharing, and circulating current minimization. Unlike conventional control algorithms, the control algorithm can guarantee not only convergence but also bounded transient tracking error. By transforming the constrained system into an unconstrained system, the transient response of DC bus voltage can always stay within user-defined, time-varying bounds. Convergence of the transformed system can meet any transient performance requirement of the original system. Through proper control effort distribution, overall load demand can be shared among the distributed generators (DGs) according to predefined percentages. Accurate load sharing can indirectly minimize the harmful circulating currents among the DGs. Switch-level simulation and hardware experimentation with both single-bus and multiple-bus DC microgrids demonstrate the effectiveness of the proposed control design.

Index Terms—DC microgrid; distributed generator; load sharing; output-constrained control; transient performance

I. INTRODUCTION

DC microgrids have been widely used in many important applications such as shipboard power systems and aircrafts [1-2]. They are generally comprised of multiple distributed generators (DGs), distributed energy storage, and loads, etc. [3]. The DC microgrid is a desirable choice for integrating the emerging DC renewable energies (e.g., photovoltaic) and DC energy storage units (e.g., batteries and supercapacitors) with DC loads (e.g., data centers) by avoiding additional AC/DC conversion stages [4]. Besides, DC microgrids also avoid the control challenges that exist in the AC microgrids, such as reference frame synchronization, system frequency evaluation

and measurement, and reactive power control [5]. One typical structure of DC microgrid is derived from connecting multiple power converter-interfaced DGs in parallel, and then supplying DC power to multiple loads through the common DC bus [6]. Once the output voltage of the common bus is well maintained, the load sharing can be realized through adjusting the output current of each DG [7].

In order to achieve reliable and efficient control of a DC microgrid, two control objectives are usually considered. The first objective is to make the common bus voltage tracking a predefined reference under various operating conditions. The voltage tracking performance plays a critical role in the loads. Conventional voltage regulation methods are mainly focused on voltage convergence instead of transient performance during the process [8-9]. Large disturbances, such as a sudden load change, may cause too much voltage overshoot or drop, which are harmful to sensitive loads and may even result in false action of the protection system [10]. The second control objective is to realize fair load sharing according to generation capability of DGs and/or system operating cost [4]. Proper load sharing is important for DGs to avoid overloading and other operational uncertainties. Accurate load sharing (output current regulation) can also help reducing circulating currents, which are currents flowing back and forth among multiple converters. Circulating currents can degrade energy efficiency, cause unbalanced load sharing, and even damage the system components [11].

In [12], a centralized control design is proposed to coordinate the parallel operation of multiple converters in a DC microgrid. The model predictive control algorithm is used for voltage regulation and load sharing. The major problem of centralized control solutions is lack of flexibility and reliability. If the system topology changes, the entire control system might have to be redesigned. Compared to distributed solutions, the centralized control solutions are more susceptible to single-point failures. Similar problems also exist with master-slave controls where voltage regulation fails under failure with the master control unit [13]. In comparison, hierarchical control scheme as proposed in [14] is more reliable where both a centralized upper-level (secondary/tertiary) control and a decentralized lower-level (primary) control are used. Even though droop control does not require inter-subsystem communications, it has some significant drawbacks, such as voltage and/or frequency deviations and limited control performance [7]. That is why droop control usually requires upper-level control to correct the deviations as introduced in [15-16].

In addition to designing advanced droop control algorithms, various non-droop control techniques, such as synergetic control, feedback linearization, backstepping and linear quadratic Gaussian, have been introduced for DC microgrids

This work was supported in part by the U.S. Office of Naval Research under Grants No. N00014-16-1-3121 and N00014-18-1-2185 and in part by the National Natural Science Foundation of China under Grants No. 61673347 and 61751205.

Cheng Wang, Jiajun Duan, and Wenxin Liu are with the Department of Electrical and Computer Engineering, Lehigh University, Bethlehem, PA 18015 USA (email: chwang925@gmail.com, jid213@lehigh.edu, wel814@lehigh.edu).

Bo Fan and Qinmin Yang are with the State Key Laboratory of Industrial Control Technology, College of Control Science and Engineering, Zhejiang University, Hanzhou, Zhejiang, 310027, China (email: kanade@zju.edu.cn, qmyang@zju.edu.cn).

controls [17-18]. In these study, algorithm analysis is usually performed based on the assumption or condition of Constant Power Loads (CPLs), which is also used in studies of automotive [19] and marine systems [2]. By considering the loads as CPLs, the control design and analysis can be significantly simplified. However, CPL is not an accurate and general model of loads, which should be better considered as a disturbance. During load changes, the algorithm designed based on CPL may still converge but the dynamic control performance will degrade significantly.

For some applications, such as military microgrids, high-performance control over bus voltage is required. However, all above control algorithms [12-19] and most conventional control solutions can only achieve converge with/without steady tracking error. They cannot guarantee that the transient tracking error before achieving steady state is bounded. As mentioned earlier, transient performance has big impacts on systems' reliability. Thus, both convergence and transient response should be properly addressed through advanced control algorithm design.

Moreover, all of above existing methods have no controllability on the transient responses so that large disturbances can be seen during the normal operating change of system [12-19], which leads to a big challenge for the protection system [10]. In this paper, a novel decentralized control algorithm is designed for the DC microgrids. The proposed control scheme integrates the function of both secondary and primary control to realize the voltage regulation and proper load sharing at the same time. The output-constrained control problem of a DC microgrid is formulated to ensure that the tracking error of voltage is always within the predefined time-varying bounds. Besides, communication-free load sharing can be realized according to the static capacities of DGs. During the control design, the original output constrained system is first transformed to an unconstrained one by using an error transformation technique. A voltage controller is then designed based on the transformed system using a backstepping method. According to the standard Lyapunov synthesis, if the convergence of the error tracking control of the transformed system can be guaranteed, the transient response of the original system will always be constrained. Once the common bus voltage converges, load sharing can be realized by adjusting the output currents of DGs. Accurate load sharing also means effective circulating current minimization. During control design, the load current is not measured to improve robustness and lower implementation difficulty.

The remaining of this paper is organized as follows. Section II presents the system model and the error constraints transformation technique of a DC microgrid. A decentralized controller with output constraint is developed in Section III. In Section IV, the effectiveness of the designed controller is verified via the detailed simulation tests using Simscape Power System toolbox of Matlab/Simulink. The hardware experiment results are given in Section V, followed by Section VI that concludes this paper.

II. SYSTEM MODELLING AND TRANSFORMATION

A. System Modeling

As shown in Fig. 1, one-bus DC microgrids with multiple parallel DGs and loads are considered [20]. Several DGs are

connected to a common DC bus through LC filters of different parameters. Due to the fast dynamic responses of converters, the system can be represented by dynamics of LC type of output filters as

$$\begin{cases} \dot{v}_o = \frac{\sum_{j=1}^n i_j}{\sum_{j=1}^n C_j} - \frac{1}{\sum_{j=1}^n C_j} i_{load} \\ \dot{i}_j = -\frac{1}{L_j} v_o - \frac{R_j}{L_j} i_j + \frac{1}{L_j} v_j, j = 1, 2, \dots, n \end{cases} \quad (1)$$

where v_o is the DC bus voltage of the system, i_{load} is total load current, i_j is the inductor current of the output filter, v_j is the control input of converter # j , L_j and C_j are inductance and capacitance of the LC output filter # j , and R_j is the parasitic resistance of the inductors.

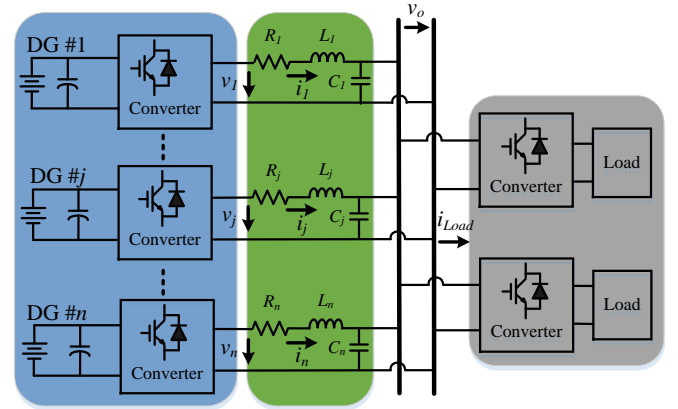


Fig. 1. The topology of a typical DC microgrid.

One major control objective of this study is to ensure the output bus voltage v_o track a desired output trajectory v_{ref} during steady operation. More strictly, the output voltage is required to stay within user-defined time-varying bounds, i.e.,

$$\underline{v}_o \leq v_o \leq \bar{v}_o \quad (2)$$

where \underline{v}_o and \bar{v}_o are the lower and upper bounds of the output voltage v_o , which can be properly defined based on the operational requirements.

Moreover, the load current $i_{load} = \sum_{j=1}^n i_j$ is also expected to be properly shared among n of DGs according to the predefined load sharing strategy, e.g., based on different capacities of DGs.

Since multiple loads might exist in a microgrid, measurement and possible communication requirement for control implementation are hard to meet. Thus, the following assumption is made to avoid the measurement difficulty.

Assumption 1: the total load current and its change rate are unknown but bounded as,

$$\begin{cases} |i_{load}| \leq I_0 \\ |\dot{i}_{load}| \leq I_1 \end{cases}$$

where I_0 and I_1 are positive constants.

B. System Transformation

Because the conventional Lyapunov function based control methodologies cannot guarantee a bounded tracking error during the transient period [21], the constrained state-space model in (1) can be transformed into an unconstrained one using a developed error transformation technique. It will be illustrated in next section that if the transformed system is stable, then both

stability and transient response of the original system can be guaranteed.

First, for the transformation, define the tracking error as

$$e_v = v_o - v_{ref} \quad (3)$$

where the output voltage reference v_{ref} is constant control reference. Since the derivative of a constant is zero ($\dot{v}_{ref} = 0$), the time derivative of the tracking error in (3) can be represented as

$$\dot{e}_v = \dot{v}_o = \frac{\sum_{j=1}^n i_j}{\sum_{j=1}^n C_j} - \frac{1}{\sum_{j=1}^n C_j} i_{load} \quad (4)$$

Then, the output bounds v_o and \bar{v}_o can be transformed into the tracking error bounds \underline{e}_v and \bar{e}_v as

$$\underline{e}_v \leq e_v \leq \bar{e}_v \quad (5)$$

where $\underline{e}_v = \underline{v}_o - v_{ref}$ and $\bar{e}_v = \bar{v}_o - v_{ref}$. Next, the constrained tracking error e_v is transformed into a new variable ξ using a user-defined transfer function,

$$\xi = T(e_v, \underline{e}_v, \bar{e}_v) \quad (6)$$

This transfer function $T(\bullet)$ needs to be smooth, strictly increasing with respect to e_v , and satisfy (7), which can be visualized in Fig. 2.

$$\left\{ \begin{array}{l} \lim_{e_v \rightarrow \bar{e}_v} \xi = +\infty \\ \lim_{e_v \rightarrow \underline{e}_v} \xi = -\infty \\ \underline{e}_v = -\bar{e}_v \\ T(0, \underline{e}_v, \bar{e}_v) = 0 \\ \text{For all } x \geq y, T(x, \underline{e}_v, \bar{e}_v) \geq T(y, \underline{e}_v, \bar{e}_v) \end{array} \right. \quad (7)$$

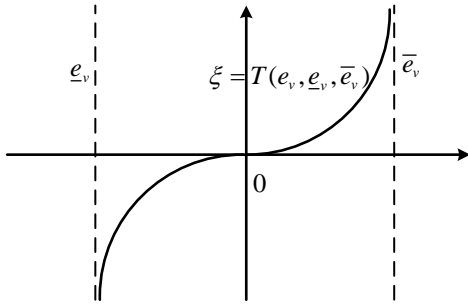


Fig. 2. The demonstration of function $\xi = T(e_v, \underline{e}_v, \bar{e}_v)$.

In this paper, the transformation function is chosen as follows, for simplicity.

$$T(e_v, \underline{e}_v, \bar{e}_v) = \text{atanh}(\alpha) \quad (8)$$

where $\alpha = \frac{2e_v - \bar{e}_v(t) - \underline{e}_v(t)}{\bar{e}_v(t) - \underline{e}_v(t)}$.

As can be seen, the transformation function in (8) satisfies all the requirements in (7). Moreover, by defining $T^{-1}(\bullet)$ as the inverse function of $T(\bullet)$ with respect to e_v , one can have

$$e_v = T^{-1}(\xi, \underline{e}_v, \bar{e}_v) \quad (9)$$

which has a unique solution when e_v is bounded according to (5). Therefore, as long as ξ exists, the output voltage tracking error e_v constraint in (5) is held. Notice that the transformation function (8) is differentiable on $e_v \in (\underline{e}_v, \bar{e}_v)$. If ξ exists, the time derivative of (6) can be expressed as

$$\dot{\xi} = a\dot{e}_v + b \quad (10)$$

where

$$\begin{cases} a = \frac{1}{1-\alpha^2} \frac{2}{(\bar{e}_v - \underline{e}_v)} \\ b = -\frac{1}{1-\alpha^2} \frac{(\bar{e}_v + \underline{e}_v)(\bar{e}_v - \underline{e}_v) + (2e_v - \bar{e}_v - \underline{e}_v)(\dot{\bar{e}}_v - \dot{\underline{e}}_v)}{(\bar{e}_v - \underline{e}_v)^2} \end{cases} \quad (11)$$

Recalling (10) and (4), the transformed system dynamics are given as

$$\begin{cases} \dot{\xi} = a \left(\frac{\sum_{j=1}^n i_j}{\sum_{j=1}^n C_j} - \frac{1}{\sum_{j=1}^n C_j} i_{load} \right) + b \\ i_j = -\frac{1}{L_j} v_o - \frac{R_j}{L_j} i_j + \frac{1}{L_j} v_j, j = 1, 2, \dots, n \end{cases} \quad (12)$$

Therefore, the original output constrained problem has been transformed into a typically unconstrained one, whose stability will be demonstrated in the following controller designs.

III. PERFORMANCE GUARANTEED CONTROLLER DESIGN

In this section, the backstepping method [22] is utilized to develop the decentralized high-performance controllers for the DC microgrids. During the controller design, two control objectives are considered and achieved together coordinately. Then the system stability is proved via the standard Lyapunov synthesis.

A. Decentralized Control Design

According to the back-stepping principle, two steps are required to develop the controller based on the transformed system dynamics in (12).

In the first step, consider the following Lyapunov function candidate

$$V_1 = \frac{\sum_{j=1}^n C_j}{2} \xi^2 \quad (13)$$

Taking the time derivative of (13) and substituting (12), it becomes

$$\begin{aligned} \dot{V}_1 &= \sum_{j=1}^n C_j \xi \dot{\xi} = \xi \sum_{j=1}^n C_j (a\dot{e}_v + b) \\ &= \xi \left[a \left(\sum_{j=1}^n i_j - i_{load} \right) + b \sum_{j=1}^n C_j \right] \end{aligned} \quad (14)$$

Now, if we define the reference of demand current for DG #j as i_j^* after the corresponding load sharing, then the output current tracking error of DG #j can be defined as

$$e_{Ij} = i_j - i_j^* \quad (15)$$

Based on (15), the total demand current reference I^* ($I^* = \sum_{j=1}^n i_j^*$) can be designed as

$$I^* = -\frac{b}{a} C - k_i \frac{\xi}{a} + \hat{i}_{load} \quad (16)$$

where $C = \sum_{j=1}^n C_j$ and k_i is a positive constant. \hat{i}_{load} is the estimation of the load current i_{load} , and its updating law follows the projection function in (17) as

$$\dot{\hat{i}}_{load} = \begin{cases} -\gamma_L a \xi, & 0 < \hat{i}_{load} < I_0 \\ 0, & \hat{i}_{load} = 0 \text{ and } \xi > 0 \\ 0, & \hat{i}_{load} = I_0 \text{ and } \xi < 0 \end{cases} \quad (17)$$

where γ_L is a positive adaption gain.

According to (18), the current reference i_j^* for each DG # j can be redesigned as

$$i_j^* = p_j I^* \quad (18)$$

where p_j is a positive constant and satisfies $\sum_{j=1}^n p_j = 1$.

It is worthwhile to mention that the current reference setting process does not require load measurement. Instead, the total demand (total injected current I^*) is calculated according to the system dynamic responses. Through proper control effort distribution, the overall load can be shared among multiple DGs. Thus, the detrimental influence of circulating currents can get minimized. The proposed load sharing method is fully decentralized and does not require any communication among different DGs.

The next step is to make subsystem injected currents track their corresponding references i_j^* s through proper design of the actual subsystem control signals.

Based on (14-18), it yields that

$$\dot{V}_1 = -k_i \xi^2 + a\xi \sum_{j=1}^n e_{Lj} - a\xi \tilde{i}_{load} \quad (19)$$

In the second step, select a new Lyapunov function candidate as

$$V_2 = V_1 + \frac{1}{2\gamma_L} \tilde{i}_{load}^2 \quad (20)$$

Recalling (19), the time derivative of V_2 can be derived as

$$\dot{V}_2 = -k_i \xi^2 + a\xi \sum_{j=1}^n e_{Lj} - a\xi \tilde{i}_{load} + \frac{1}{\gamma_L} \tilde{i}_{load} \left(\dot{i}_{load} - \hat{i}_{load} \right) \quad (21)$$

Based on the Assumption 1 and (17), it follows that

$$\dot{V}_2 \leq -k_i \xi^2 + a\xi \sum_{j=1}^n e_{Lj} + \frac{2I_0 I_1}{\gamma_L} \quad (22)$$

Next, consider the following augmented Lyapunov function V_3

$$V_3 = V_2 + \frac{1}{2} \left(\sum_{j=1}^n e_{Lj} \right)^2 \quad (23)$$

Recalling (22), the first derivative of (23) can be written as

$$\dot{V}_3 \leq -k_i \xi^2 + \frac{2I_0 I_1}{\gamma_L} + \sum_{j=1}^n e_{Lj} \sum_{j=1}^n \left(\frac{a\xi}{n} - \frac{1}{L_j} v_o - \frac{R_j}{L_j} i_j + \frac{1}{L_j} v_j - i_j^* \right) \quad (24)$$

Based on (24), the controller for DG # j can be designed as

$$v_j = R_j i_j + v_o + L_j i_j^* - k_v L_j e_{Lj} - \frac{1}{n} L_j a \xi \quad (25)$$

It should be noted that the control input in (25) is designed based on the final global Lyapunov function defined in (23). The local control signal defined in (25) is able to guarantee the derivative of V_3 in (24) is negative definite. Since v_j can be calculated using local signals only, the fully decoupled control block diagram of the subsystem is illustrated as Fig. 3. First, states of the original system are measured and transformed for output constraint control design. Then, the overall injected current (overall control effort) for bus voltage control is calculated and shared among multiple DGs. Finally, an output-constrained controller is utilized to realize the desired load sharing as well as the high-performance voltage regulation.

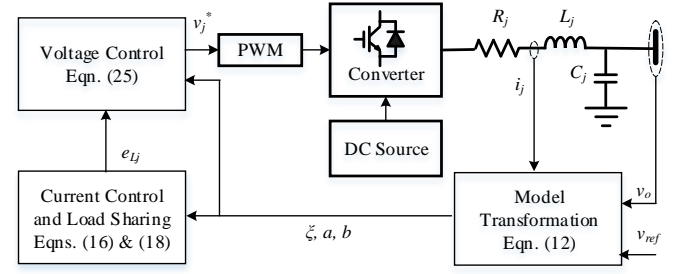


Fig. 3. Closed-loop block diagram of the proposed control scheme.

B. Stability Analysis

Theorem 1 (Voltage Regulation and Load Sharing Control Design): Under the assumption 1, using the controller designed in (21), the voltage regulation and the load sharing (based on p_j) can be realized. Besides, the stability of the system can also be guaranteed.

Proof: See Appendix.

IV. SIMULATION STUDIES

A. System Definition

The proposed control scheme is tested with a 3 kW, one-bus, four-DG DC microgrid simulated with Simscape Power System toolbox of Matlab/Simulink. To challenge the control algorithm, different filter parameters, various loading conditions, and both even and uneven load sharing are simulated. The total simulation time is 0.25 s under a sampling rate of 0.1 ms. Instead of testing under a constant power load, a larger load change and smaller load change are simulated at time $t=0.05$ s and $t=0.15$ s, respectively, to evaluate the proposed control algorithm under disturbances. The bus voltage reference (v_{ref}) is 120 V. The model and control parameters for simulation studies are presented in Table I.

TABLE I
PARAMETERS OF THE TEST SYSTEM

Item	Specification
Output resistors (R_1, R_2, R_3, R_4)	0.21, 0.2, 0.2, 0.19 Ω
Output inductors (L_1, L_2, L_3, L_4)	2.1, 2.0, 2.0, 1.9 mH
Output capacitors (C_1, C_2, C_3, C_4)	25, 25, 25, 25 μ F
DC load	10 Ω (before 0.05s); 5 Ω (after 0.05s); 6 Ω (after 0.15s)
k_i	1
k_v	500
γ_L	400

The dynamic output error bounds are defined as:

$$\bar{e}_v = -\underline{e}_v = A + b e^{-\frac{t-t^*}{\tau}} \quad (26)$$

where A , b and τ are user-defined constants and t^* is the instant of time when the time-varying boundary function is reinitialized due to large disturbance.

During normal operation, small disturbances always exist. To reduce control effort, the voltage error bound can be held constantly under small disturbances. Only large load changes that make bus voltage go beyond a predefined bound will trigger updating output error bound.

B. Case I: Evenly Load Sharing

In this case, four DGs are designed to evenly share the 12 A load current while $0 \leq t < 0.05$ s, 24 A while $0.05 \leq t < 0.15$ s,

and 20 A afterward. Correspondingly, each DG should generate 3.0 A, 6.0 A and 5.0 A output current during three periods. The parameters of the transient bound function are set according to $A=4.8$, $b=7.2$ and $\tau=1/240$ to limit transient output voltage during normal operating condition.

In order to better evaluate the performance of the proposed controller, a droop-based PI controller proposed in [24] is utilized for comparison. The droop equation is given as

$$v_{ref} = v_n - d_j i_j + k_j i_{load} \quad (27)$$

where v_n is the nominal voltage. $i_{load} = \sum_{j=1}^n i_j$ represents the total output current. d_j and k_j are the positive droop gain which is decided by the load sharing property and satisfy $d_j k_j > 0$.

For convenience, the control diagram of the droop and PI based controller is shown in Fig. 4. It should be noted that total load measurement is required for load sharing. The PI gains used in the simulation have been well-tuned using the classic Ziegler-Nichols method [25] and are listed in Table II. It should be noted that PI control might provide better performance. However, tuning multiple ($n \times 6$) parameters based on different LC filters is very difficult. In addition, the well-tuned PI parameters for one operating condition may not work well for another operating condition.

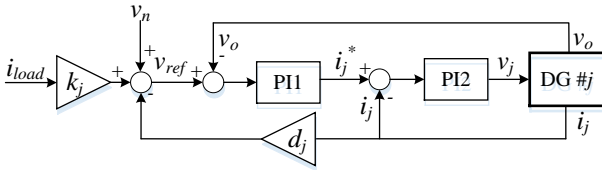


Fig. 4. Block diagram of a droop-based PI controller.

TABLE II
PARAMETERS OF THE DROOP-BASED PI CONTROLLER

Item	Specification
Proportional Gain of PI1	1
Integral Gain of PI1	80
Proportional Gain of PI2	1
Integral Gain of PI2	800
d_j	5
k_j (even load sharing)	1.25
k_j (proportional load sharing)	1.0, 1.25, 1.25, 1.5

In simulation studies, the best control performance of a PI control is presented at first. Then, a tighter bound is designed and the proposed control algorithm is used to overbear the control performance of PI. The system responses under droop-PI controller and the proposed output-constraint controller are shown in Fig. 5-7.

As can be seen in Fig. 5, a significant load change causes large disturbance to the output voltage v_o . Even if droop-PI control can stabilize bus voltage, there is still room for improvement of transient responses. In Fig. 5(a), one can see that the overshoot is larger than 12 V (10% of v_n) and it takes about 0.04 s to converge. In comparison, the proposed algorithm can provide much better transient performance due to the stringent output constraints. Both overshoot and time of convergence become smaller. Eventually, the transient bound converges to a nonzero constant that is used to tolerate small disturbances. And control efforts still exist even under constant bound.

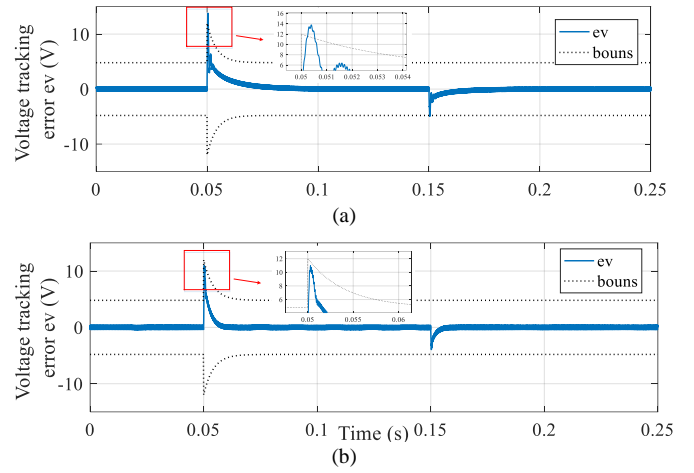


Fig. 5. The responses of output voltage tracking error e_v under evenly load sharing condition: (a) PI controller; (b) proposed controller.

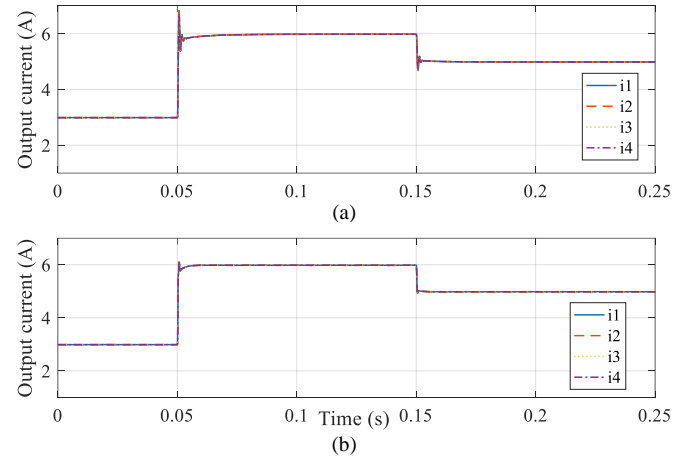


Fig. 6. The responses of output current i_j under evenly load sharing condition: (a) PI controller; (b) proposed controller.

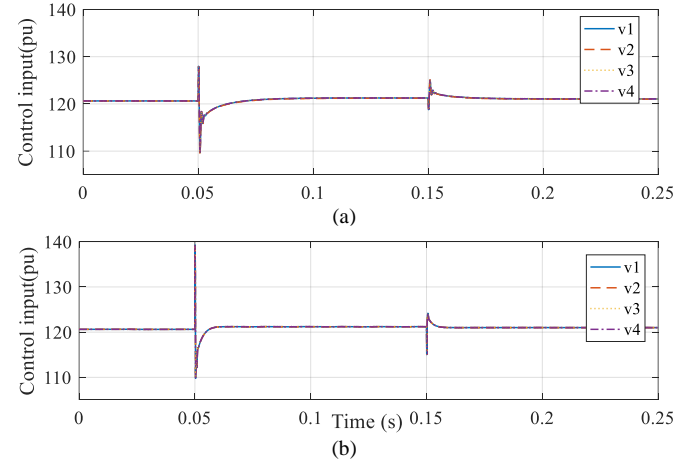


Fig. 7. The responses of control input v_j under evenly load sharing condition: (a) PI controller; (b) proposed controller.

From Fig. 6, one can see that both algorithms can realize accurate even load sharing. However, the droop-PI control causes a larger transient response and takes a longer time to converge than the proposed control due to the limited voltage performance. The proposed control design can generate better control signals that can damp out disturbances on output voltage in a fast and accurate way, which can effectively eliminate

circulating currents during the transient stage. As shown in the experimental study, the control signals, even though large, can be successfully realized by PWM converters.

C. Case II: Uneven Load Sharing

In the second case, the proportional load sharing control is performed. During the test, the capacity ratio of four DGs are set to be 20%, 25%, 25% and 30%. Therefore, it means that the output current references i_j^* are 2.4 A, 3.0 A, 3.0 A and 3.6 A, respectively, while $0 \leq t < 0.05$ s; 4.8 A, 6.0 A, 6.0 A and 7.2 A, respectively, while $0.05 \leq t < 0.15$ s; and 4.0 A, 5.0 A, 5.0 A and 6.0 A, respectively, while $0.15 \leq t$. The rest of system settings are same as the previous case.

The system responses under droop-PI controller and the proposed output-constraint controller are shown in Fig. 8-10. Again, the transient performance of PI controller during the load change is limited and a large voltage overshoot can be observed in Fig. 8(a). In addition, the droop-based PI controller has a slight steady-state error of output currents i_j s under the proportional load sharing condition as shown in Fig. 9(a). This error is due to the unbalanced system parameters, which has been well discussed in [23]. Even if this error can be compensated by tuning the droop gains based on the system parameters dynamically [23], it is not easy to be implemented and more complex algorithms might have to be used.

On the contrary, the proposed controller can still maintain the voltage deviation e_v within the predefined bounds \bar{e}_v and \underline{e}_v rigorously under the proportional load sharing condition as shown in Fig. 8(b). In addition, output currents i_j s can achieve the proportional load sharing accurately as presented in Fig. 9(b). Then the control inputs comparison is shown in Fig. 10.

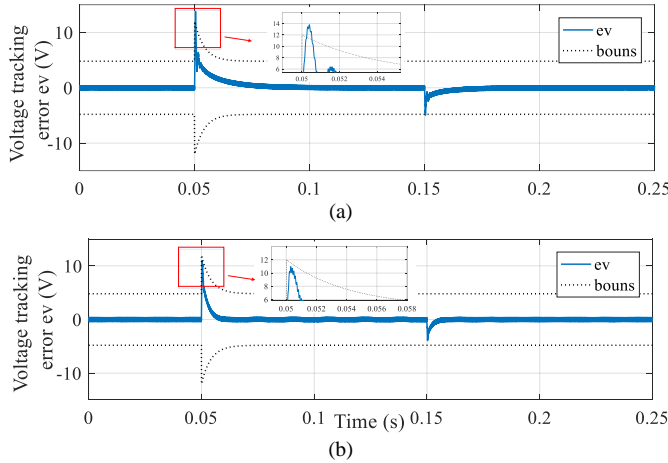


Fig. 8. The responses of output voltage tracking error e_v under proportional load sharing condition: (a) PI controller; (b) proposed controller.

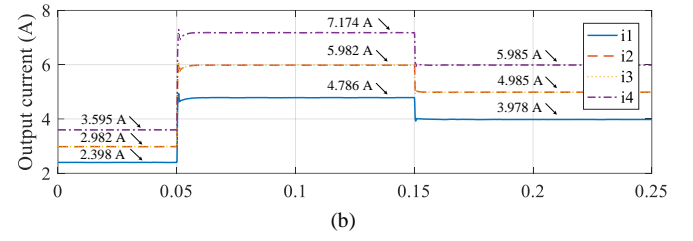
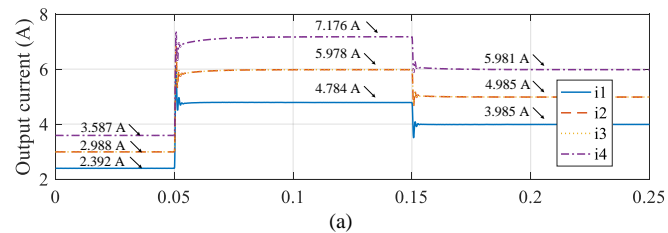


Fig. 9. The responses of output current i_j under proportional load sharing condition: (a) PI controller; (b) proposed controller.

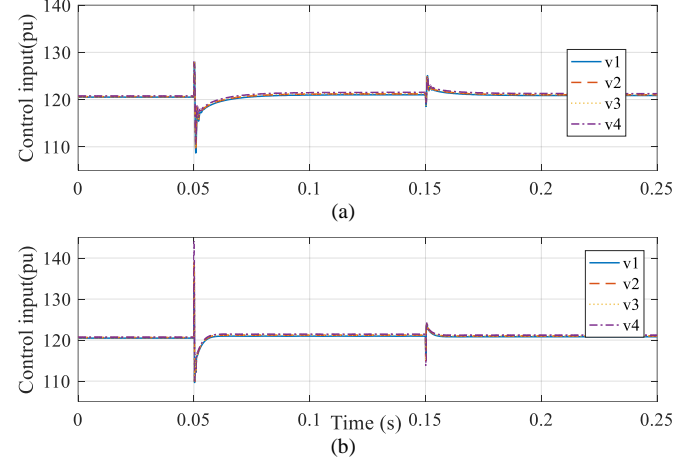


Fig. 10. The responses of control input v_j under proportional load sharing condition: (a) PI controller; (b) proposed controller.

V. EXPERIMENT RESULTS

Our lab has developed a power converter based experimental platform for the integrated study of power and controls. The modular converts can be flexibly configured to form different topology and controlled by dual-core DSP control boards. To test the proposed control algorithm, a two-bus DC microgrid is configured as shown in Fig. 11. Subsystem #1 has two DGs (DG₁ and DG₂) and Subsystem #2 has one DG (DG₃). Each DG is implemented with a DC power supply, a modular power converter, and LC output filter. A resistive load bank is connected to Bus1. Each DG is controlled by a control board that has both DSP (TI- TMS320C28346) and FPGA (Cyclone IV). The control algorithm is implemented with the DSP and the PWM is generated with the FPGA. The picture of actual hardware setup is shown in Fig. 12 and the key parameters and operating conditions are listed in Table III. One can see that the filter parameters are made different from each other to challenge the designed control algorithm.

TABLE III PARAMETERS OF MICROGRID DURING THE EXPERIMENT

Parameters	Value
Filter resistance (R_1, R_2, R_3)	0.1, 0.2, 0.3 Ω
Filter inductance (L_1, L_2, L_3)	2.1, 2.2, 2.0 mH
Filter capacitance (C_1, C_2, C_3)	25, 25, 25, 25 μ F
Line resistance (R_l)	0.5 Ω
Load	200W (1 p.u.)

The switch in Fig. 11 can connect and disconnect the two subsystems to test the proposed algorithm in different applications (one-bus or multiple-bus DC microgrids). The proposed algorithm is first tested with a single subsystem #1 that

has multiple (two) DGs. Afterwards, it is tested with two subsystems to evaluate its possible application with larger-scale microgrids. Corresponding experimental results are shown in Fig. 13 and Fig. 14, respectively.

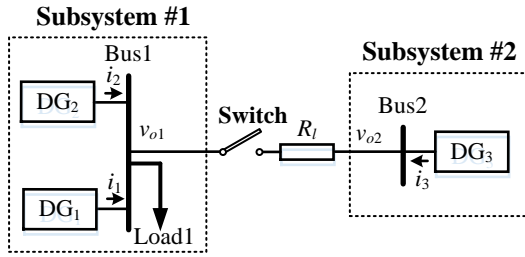


Fig. 11. The topology of DC microgrid with two clusters in experiment.

Fig. 13(a) shows system responses under change of load sharing demand from even (1:1) to uneven (2:3) load sharing due to change of generation capacities at t_1 . The demand for change of load sharing ratio can be accomplished in a fast and smooth manner. During this process, the voltage only has very small oscillations because the load resistance is held fixed. In Fig. 13(b), the load sharing ratio is changed at t_2 again to 4:3, which causes the generation curves of the DGs switching over. Again, one can see that load sharing demand can be realized accurately with very small disturbances on bus voltage.

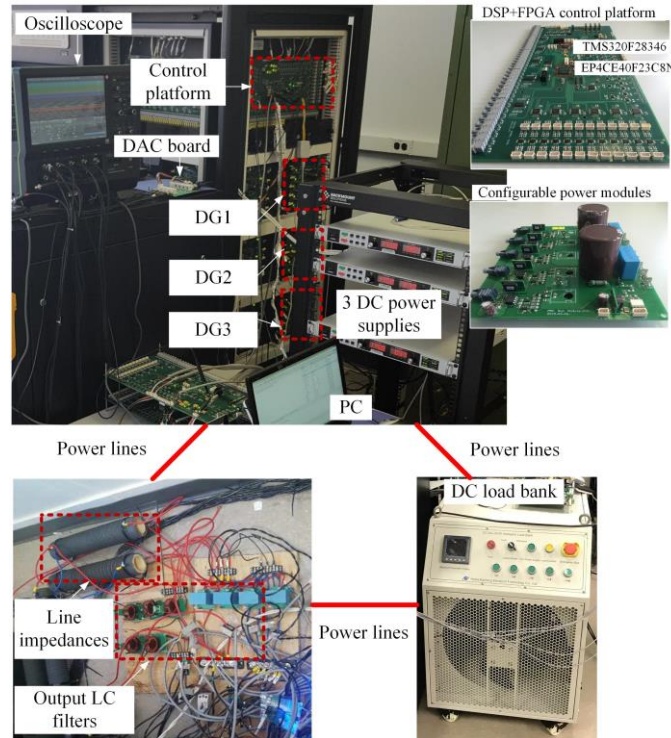


Fig. 12. Experimental setup.

To apply the designed algorithm to a multiple-bus DC microgrid, a secondary control algorithm is needed to decide the voltage references for multiple buses. Many secondary control algorithms can be introduced for this purpose [27]. To maintain stability under disturbances and uncertainties, a conventional droop control method is introduced to adjust voltage references between reference update [27]. During experimentation, the two-bus microgrid is started at t_3 . Since the load sharing

performance under constant load has been tested with one-bus microgrid through hardware experimentation, the objective of this experiment is to evaluate control performance of multiple-bus microgrid under load change. During the experiment, a load decrease and a load increase are performed at t_4 and t_5 , respectively. Under both conditions, the bus voltages are well controlled with very small disturbances. In addition, even load sharing can also be achieved but with small deviations. The deviation is mainly caused by droop control and can be eliminated by deploying advanced secondary control algorithms.

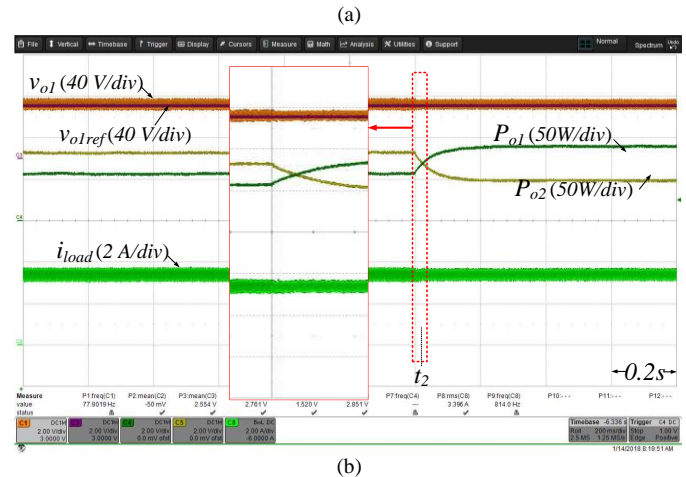
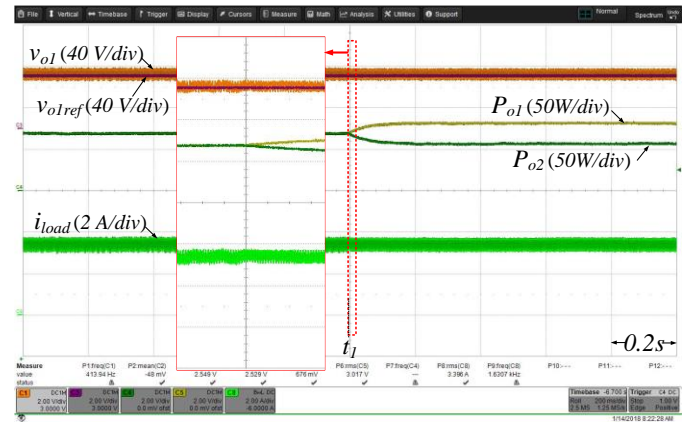


Fig. 13. Experiment results of one-bus DC microgrid: (a) transition from even to uneven load sharing (2:3); (b) transition from one load sharing ratio (2:3) to another (4:3).

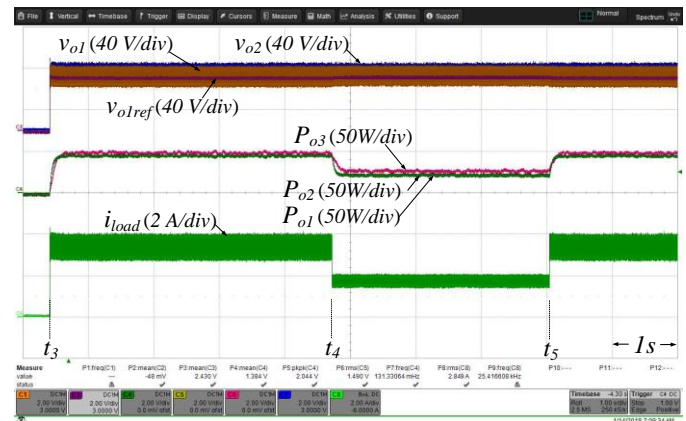


Fig. 14 Experiment results of two-bus DC Microgrid.

VI. CONCLUSION

DC microgrids have been widely used in many critical applications. The effective control is very important to maintain the system output stay bounded during both transient and steady states. In this paper, a high-performance control scheme is proposed for DC microgrids. Through model transformation, the original output constrained model is transformed into an unconstrained one. By using the backstepping method, a voltage regulator is designed which can guarantee the transient tracking error always staying within user-defined time-varying bounds. In the meantime, the proper load sharing can be achieved as the output voltage converges. All closed-loop signals are proved to be bounded according to standard Lyapunov synthesis. The effectiveness of the proposed algorithm has been tested through extensive simulations as well as hardware experiments with both single- and multiple bus DC microgrid. In the future, adaptive and robust control algorithms can be designed to address the system uncertainties. More advanced secondary control algorithms can also be integrated to extend the applications to multiple-bus microgrid and to realize dynamic load sharing.

APPENDIX

Proof of Theorem 1

First, substituting (25) into (24), one can have

$$\dot{V}_3 \leq -k_i \xi^2 - k_v \sum_{j=1}^n e_{Lj}^2 + \frac{2I_0 I_1}{\gamma_L} \quad (\text{A.1})$$

Then, recalling the Lyapunov functions in (13), (20), (23), it yields

$$V_3 = \frac{C}{2} \xi^2 + \frac{1}{2\gamma_L} \tilde{i}_{load}^2 + \frac{1}{2} \left(\sum_{j=1}^n e_{Lj} \right)^2 \quad (\text{A.2})$$

Then it can be derived that

$$\dot{V}_3 \leq -c_1 V_3 + c_2 \quad (\text{A.3})$$

where $c_1 = \min \left\{ \frac{2k_i}{C}, 2k_v \right\}$ and $c_2 = \frac{2I_0 I_1}{\gamma_L} + \frac{2c_1}{\gamma_L} I_0^2$.

According to the Lyapunov synthesis [21], one can conclude that all of the signals in the closed-loop system (12) are bounded. Furthermore, the proposed control law (25) can guarantee that [21]

$$\lim_{t \rightarrow \infty} V_3(t) \leq \frac{c_2}{c_1} \quad (\text{A.4})$$

which implies that the transformed voltage error and current error can be made arbitrarily small by properly tuning of control gains.

Combined with the definition of system transformation, the original voltage error is guaranteed to stay within the bounds. Therefore, both voltage regulation and load sharing can be achieved.

REFERENCES

- [1] D. Bosich, G. Giadrossi, and G. Sulligoi, "Voltage control solutions to face the CPL instability in MVDC shipboard power systems," in *AEIT Annual Conference*, Trieste, Italy, Sept. 2014, pp. 1-6.
- [2] P. Magne, B. Nahid-Mobarakeh, and S. Pierfederici, "Active stabilization of DC microgrids without remote sensors for more electric aircraft," *IEEE Transactions on Industry Applications*, vol. 49, no. 5, pp. 2352-2360, 2013.
- [3] W. Su, and J. Wang, "Energy management systems in microgrid operations" *The Electricity Journal*, vol. 25, no. 8, pp. 45-60, 2012.

- [4] Y. Chen, Y. Wu, C. Song, and Y. Chen, "Design and implementation of energy management system with fuzzy control for DC microgrid systems," *IEEE Transactions on Power Electronics*, vol. 28, no. 4, pp. 1563-1570, 2013.
- [5] J. Duan, C. Wang, H. Xu, and W. Liu, Y. Xue, J. Peng, and H. Jiang, "Distributed control of inverter-interfaced microgrids based on consensus algorithm with improved transient performance," *IEEE Transactions on Smart Grid*, Early Access, 2017.
- [6] L. Herrera, W. Zhang, and J. Wang, "Stability analysis and controller design of DC microgrids with constant power loads," *IEEE Transactions on Smart Grid*, Early Access, 2015.
- [7] A. Tah and D. Das, "An enhanced droop control method for accurate load sharing and voltage improvement of isolated and interconnected DC microgrids," *IEEE Transactions on Sustainable Energy*, vol. 7, no. 3, pp. 1194-1204, 2016.
- [8] A. Khorsandi, M. Ashourloo, and H. Mokhtari, "A decentralized control method for a low-voltage DC microgrid," *IEEE Transactions on Sustainable Energy*, vol. 7, no. 3, pp. 1194-1204, 2016.
- [9] B. Fan, Q. Yang, K. Wang, J. Xu, and Y. Sun, "Transient stability enhancement control of power systems with time-varying constraints," *IET Generation, Transmission & Distribution*, vol. 10, no. 13, pp. 3251-3263, 2016.
- [10] C. Christopoulos, and A. Wright, *Electrical Power System Protection*, Springer Science & Business Media, 1999.
- [11] T. Wu, Y. Chen, and Y. Huang, "3C strategy for inverters in parallel operation achieving an equal current distribution," *IEEE Transactions on Industrial Electronics*, vol. 47, no. 2, pp. 273-281, 2000.
- [12] K. Tan, X. Peng, P. So, Y. Chu, and M. Chen, "Centralized control for parallel operation of distributed generation inverters in microgrids," *IEEE Transactions on Smart Grid*, vol. 3, no. 4, pp. 1977-1987, 2012.
- [13] S. K. Mazumder, M. Tahir, and K. Acharya, "Master-slave current sharing control of a parallel dc-dc converter system over an RF communication interface," *IEEE Transactions on Industrial Electronics*, vol. 55, no. 1, pp. 59-66, 2008.
- [14] J. Guerrero, J. Vasquez, J. Matas, L. Vicuna, and M. Castilla, "Hierarchical control of droop-controlled AC and DC microgrids-A general approach toward standard," *IEEE Transactions on Industrial Electronics*, vol. 58, no. 1, pp. 158-172, 2011.
- [15] A. Khorsandi, M. Ashourloo, H. Mokhtari, and R. Iravani, "Automatic droop control for a low voltage DC microgrid," *IET Generation, Transmission & Distribution*, vol. 10, no. 1, pp. 41-47, 2016.
- [16] Y. Gu, X. Xiang, W. Li, and X. He, "Mode-adaptive decentralized control for renewable DC microgrid with enhanced reliability and flexibility," *IEEE Transactions on Power Electronics*, vol. 29, no. 9, pp. 5072-5080, 2014.
- [17] M. Cupelli, M. Moghimi, A. Riccobono, and A. Monti, "A comparison between synergetic control and feedback linearization for stabilizing MVDC microgrids with constant power load," in *IEEE PES Innovative Smart Grid Technologies*, Istanbul, Turkey, Oct. 2014, pp. 1-6.
- [18] M. Cupelli, M. Mirz, and A. Monti, "A comparison of backstepping and LQG control for stabilizing MVDC microgrids with constant power loads," in *2015 IEEE Eindhoven PowerTech*, Eindhoven, Netherlands, July 2015, pp. 1-6.
- [19] A. Emadi, A. Khaligh, C. Rivetta, and G. Williamson, "Constant power loads and negative impedance instability in automotive systems: Definition, modeling, stability, and control of power electronic converters and motor drives," *IEEE Transactions on Vehicular Technology*, vol. 55, no. 4, pp. 1112-1125, 2006.
- [20] K. Low, and R. Cao, "Model predictive control of parallel-connected inverters for uninterruptible power supplies," *IEEE Transactions on Industrial Electronics*, vol. 55, no. 8, pp. 2884 - 2893, 2008.
- [21] P. Giesl, *Construction of Global Lyapunov Functions Using Radial Basis Functions*, Springer Berlin Heidelberg, 2007.
- [22] M. Krstic, P. Kokotovic, and I. Kanellakopoulos, *Nonlinear and Adaptive Control Design*. John Wiley & Sons, Inc., 1995.
- [23] W. Yao, M. Chen, J. Matas, J. Guerrero, and Z. Qian, "Design and analysis of the droop control method for parallel inverters considering the impact of the complex impedance on the power sharing," *IEEE Transactions on Industrial Electronics*, vol. 58, no. 2, pp. 576 - 588, 2011.

- [24] S. Anand, B. Fernandes, and J. Guerrero, "Distributed control to ensure proportional load sharing and improve voltage regulation in low-voltage DC microgrids," *IEEE Transactions on Power Electronics*, vol. 28, no. 4, pp. 1900-1913, 2013.
- [25] F. A. Salem and A. A. Rashed, "PID controllers and algorithms: selection and design techniques applied in mechatronics systems design," *International Journal of Engineering Sciences*, vol. 2, no. 5, pp. 191-203, 2013.
- [26] Y. Zhang, M. Yu, F. Liu, and Y. Kang, "Instantaneous current-sharing control strategy for parallel operation of UPS modules using virtual impedance," *IEEE Transactions on Power Electronics*, vol. 28, no. 1, pp.432-440, 2013
- [27] J.M. Guerrero, J.C. Vasquez, J. Matas, L.G. De Vicuña, and M. Castilla, "Hierarchical control of droop-controlled ac and dc microgrids-a general approach toward standardization," *IEEE Transactions on Industrial Electronics*, vol. 58, no. 1, pp. 158-172, 2011.



Cheng Wang (S'12) received the B.S. degree in electrical engineering from Southwest Jiaotong University, Chengdu, China in 2011, and is currently working toward the Ph.D. degree in electrical engineering in the School of Electrical and Electronics Engineering, Huazhong University of Science and Technology at Wuhan, China. He is also a research assistant with the Department of Electrical and Computer Engineering, Lehigh University at PA, USA. His research interests include Microgrids, high penetrative grid-interactive photovoltaic system, modular multilevel converters and uninterrupted power systems.



smart microgrid.

Jiajun Duan (S'14) was born in Lanzhou, China, in 1990. He received his B.S. degree in Power system and its automation from Sichuan University, Chengdu, China, and M.S. degree in in Electrical Engineering at Lehigh University, Bethlehem, PA in 2013 and 2015, respectively. He is currently pursuing the Ph.D. degree at Lehigh University. His research interest includes power system, power electronics, control systems, renewable energy and



nonlinear system theory and renewable energy systems.

Bo Fan (S'15) received the Bachelor's degree in Automation from the Zhejiang University, Hangzhou, China in 2014. He is currently working toward the Ph.D. degree in Control Science and Engineering at Zhejiang University, Hangzhou, China. He is a member of the Group of Networked Sensing and Control (IIPC-NeSC), State Key Laboratory of Industrial Control Technology, Zhejiang University. His research interests include



Professor with the Department of Electrical and Computer Engineering, Lehigh University, Bethlehem, PA, USA. His research interests include power systems, power electronics, and controls.

Wenxin Liu (S'01-M'05-SM'14) received the B.S. degree in industrial automation, and the M.S. degree in control theory and applications from Northeastern University, Shenyang, China, in 1996 and 2000, respectively, and the Ph.D. degree in electrical engineering from the Missouri University of Science and Technology (formerly University of Missouri-Rolla), Rolla, MO, USA, in 2005. Currently, he is an Assistant



Research Associate at University of Missouri-Rolla. In 2008, he was a system engineer with Caterpillar Inc. From 2009 to 2010, he was a Post-doctoral Research Associate at University of Connecticut. Since 2010, he has been with the State Key Laboratory of Industrial Control Technology, the Department of Control Science and Engineering, Zhejiang University, China, where he is currently an associate professor. His research interests include intelligent control, renewable energy systems, nano-robotics, and system diagnosis.

Qinmin Yang (M'10) received the Bachelor's degree in Electrical Engineering from Civil Aviation University of China, Tianjin, China in 2001, the Master of Science Degree in Control Science and Engineering from Institute of Automation, Chinese Academy of Sciences, Beijing, China in 2004, and the Ph.D. degree in Electrical Engineering from the University of Missouri-Rolla, MO USA, in 2007. From 2007 to 2008, he was a Post-doctoral